

Evidence of a Higher-Order Singularity in Dense Short-Ranged Attractive Colloids

Francesco Sciortino, Piero Tartaglia, and Emanuela Zaccarelli

Dipartimento di Fisica, INFN Udr and Center for Statistical Mechanics and Complexity, Università di Roma La Sapienza, I-00185 Rome, Italy

(Received 7 April 2003; published 29 December 2003)

We study a model in which particles interact through a hard-core repulsion complemented by a short-ranged attractive potential of the kind found in colloidal suspensions. Combining theoretical and numerical work we locate the line of higher-order glass-transition singularities and its end point—named A_4 —on the fluid-glass line. Close to the A_4 point, we detect logarithmic decay of density correlations and a sublinear power-law increase of the mean square displacement, for time intervals up to 4 orders of magnitude. We establish the presence of the A_4 singularity by studying how the range of the potential affects the time window where anomalous dynamics is observed.

DOI: 10.1103/PhysRevLett.91.268301

PACS numbers: 82.70.Dd, 64.70.Pf, 83.80.Uv

Recently, a great deal of interest has grown around dynamical phenomena arising in dense colloidal suspensions when particles interact through a hard-core repulsion followed by a rather short-ranged attractive potential [1–3]. Some of these unusual phenomena, initially predicted theoretically [4–6], have been observed experimentally [7–10] and in numerical simulations [11–15]. The novelty, as compared to the well-studied hard-sphere-colloids case, comes from the possibility of generating structurally arrested states with an additional physical mechanism, driven by the range of the attractive interaction. Indeed, in the case of hard sphere, structural arrest is controlled by the well-known excluded volume cage effect, where particle motion is hindered by the presence of neighboring ones. This mechanism generates a localization length of the order of 10% of the particle diameter σ . In the additional mechanism, the motion of the particles is restricted by the adhesiveness, i.e., the formation of nonpermanent bonds due to the attractive part of the interparticle potential; particles are confined by bonds and the corresponding localization length is fixed by the attraction range Δ . When $\Delta \ll \sigma$, the interplay of the two localization mechanisms creates liquid states for packing fractions higher than those possible for a pure hard-sphere system. This means that the attraction stabilizes the liquid and leads to a reentry phenomenon, where this new liquid state can arrest into a glass by cooling as well as heating. The experimental and numerical confirmation of this prediction [9–14] suggests that the mode-coupling theory (MCT) [16], which was the basis of the cited theoretical work [4–6], can contribute to explain the slow dynamics in short-ranged attractive colloids.

These systems are characterized by three control parameters—the packing fraction ϕ , the ratio θ of the thermal energy $k_B T$ to the typical well depth u_0 , and the range Δ of the attractive potential. Within MCT, the phase diagram of this three-dimensional control-parameter space (shown in Fig. 1) is organized around a

critical point $(\phi^*, \theta^*, \Delta^*)$, referred to as a type A_4 higher-order glass-transition singularity in MCT classification. A_4 is the end point of a line of higher-order singularities (of type A_3). From a physical point of view, A_4 is characterized for being the only singularity point accessible from the liquid phase. For $\Delta > \Delta^*$ no singular points are predicted by the theory, while for $\Delta < \Delta^*$ the A_3 singularity points are buried in the glass phase, and their presence can be observed only indirectly [7,9,11,14]. Near the A_4 singularity, MCT predicts a structural relaxation dynamics, which is utterly different from that known for conventional glass-forming liquids. It is ruled

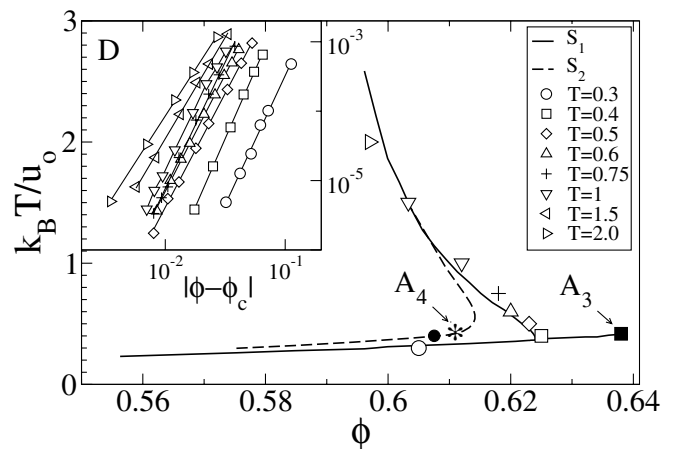


FIG. 1. Glass transition line for the system S_1 calculated through the vanishing of the diffusion (open symbols) and calculated with MCT (full line). The MCT ideal glass line for S_2 is given by the dashed line. The star indicates the location of the A_4 singularity (on the S_2 ideal glass line) while a filled square locates the A_3 point (on the S_1 line). The MCT curves have been transformed according to the mapping discussed in the text. The T and ϕ of the simulated point are indicated by the black dot. The inset shows the power-law fits for the isothermal diffusion coefficient D (data from Ref. [14]) for S_1 as a function of $\phi - \phi_c$ (see text).

by logarithmic variations of correlators as a function of time and subdiffusive increase of the mean squared displacement (MSD). Theory makes precise predictions for the time interval where this unusual dynamics is expected, as well as for its variation with changes of the ϕ , θ , and Δ parameters. Indications of logarithmic dynamics have been reported [7,9,11,14], but neither a systematic study of the dependence on the control parameters has been published nor the A_4 point has been located numerically. It is, in fact, difficult to discriminate between straight lines caused by some inflection points in the usual logarithmic representation of correlators and the logarithmic decay laws generated by the higher-order singularity. In this Letter, we establish the existence of the location of the A_4 point for a well defined model, amenable of simultaneous numerical and theoretical treatment. Reported data—with control parameters explicitly chosen close to the A_4 point—exhibit the mentioned laws over time intervals up to 4 orders of magnitude. More importantly, we show that the decay patterns vary with changes of the control parameters and wave vectors as expected [17,18], properly testing the theoretical predictions.

We simulate a 50%–50% binary mixture of $N = 700$ hard spheres of mass m , with diameters σ_{AA} and σ_{BB} and ratio $\sigma_{AA}/\sigma_{BB} = 1.2$. The hard core between particles of different type $\sigma_{AB} = 0.5(\sigma_{AA} + \sigma_{BB})$. The hard-core potential is complemented by an attractive square-well potential of depth u_o , independent of the particle type [19]. The small asymmetry in the diameters is sufficient to prevent crystallization at high values of ϕ . We focus on two specific systems, which we label S_1 and S_2 , differing in the width of the square well Δ_{ij} . S_1 and S_2 have $\Delta_{ij} = 0.031\sigma_{ij}$ and $\Delta_{ij} = 0.043\sigma_{ij}$, respectively ($i = A, B$). The system S_1 has been extensively studied in previous simulations [14]. As discussed in the following, S_2 is chosen to coincide with the critical amplitude parameter within the accuracy of our calculations. Averages over five independent realizations have been performed to reduce noise. Equilibration has been carefully checked. We note that our results refer to Newtonian dynamics, but are relevant also to Brownian dynamics in the structural relaxation time window [20].

To estimate the predicted location of the A_4 point for the binary mixture square-well model (and consequently select the parameters to be used in the simulations), we proceed as follows. First, we calculate the glass line $\phi_c(T)$ for the mixture S_1 extrapolating diffusivity D data [14] according to $D \sim [\phi - \phi_c(T)]^{\gamma(T)}$, for eight different T . Second, we calculate the MCT ideal glass-transition line. The partial structure factors, the only input needed, are calculated with the Percus-Yevick approximation, numerically solving the Ornstein-Zernike equation [21]. Third, we map the theoretical glass line on the simulation line, following the procedure first used by Sperrl [18]. Indeed, MCT cannot reproduce the numerical

values for ϕ_c . As shown in Fig. 1, the linear transformation $\phi \rightarrow 1.897\phi - 0.3922$ and $T \rightarrow 0.5882T - 0.225$, allows one to superimpose the MCT result with the simulation data, in the studied region of T and ϕ . By calculating the MCT ideal glass-transition line for several values of Δ , the theoretical location of the A_4 point for the binary mixture square-well model is obtained. Assuming that, to a first approximation, the same linear transformation holds also for the critical value of the well width, we find that the A_4 location maps to $\Delta_{ij}^* = 0.043\sigma_{ij}$, $\phi^* = 0.611$, and $\theta^* = 0.416$. This allows us to select a state point with parameters close to the critical ones and perform a simulation (in thermodynamic equilibrium) close to A_4 . We choose [22] $\theta = 0.4$ and $\phi = 0.6075$ and compare, for the same T and ϕ , the dynamics for Δ_{ij}^* (system S_2) and for the close-by value $\Delta_{ij} = 0.031\sigma_{ij}$ (S_1).

Figure 2 shows the MSD for the larger species $\langle \delta r_A^2 \rangle$ for both systems. We notice the presence of a subdiffusive regime at intermediate times, i.e., a variation according to $\ln(\langle \delta r_A^2 \rangle) = f + a \ln(t/\tau)$ for about 3 decades for S_1 , where $a_1 = 0.44$. The logarithmic regime extends by more than a decade if the attraction range is increased to that for system S_2 . Simultaneously the exponent a decreases to $a_2 = 0.28$. Figure 3 shows the density-fluctuation autocorrelation functions $\Phi_q(t)$ for a representative set of wave vectors q . The decay curves in Fig. 3 do not show the two steps scenario with a plateau characteristic of conventional glass-forming liquids. Indeed, it is impossible to fit these curves for large q with the standard stretched exponential function. Instead, there is a region of clear logarithmic decay at $q_1^*\sigma_{BB} = 23.5$ for S_1 and at $q_2^*\sigma_{BB} = 16.8$ for S_2 . The time intervals over which logarithmic decay is observed are of similar size as those for the MSD. For $q < q^*$, the Φ_q vs $\ln t$ curves are concave, and for $q > q^*$ convex.

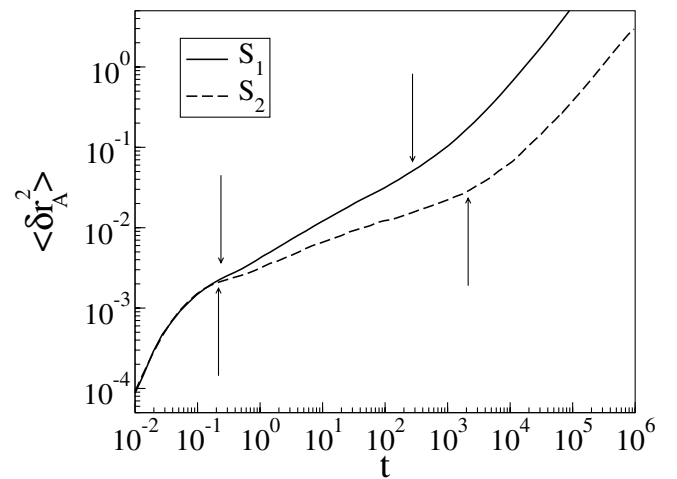


FIG. 2. Mean squared displacement of the A particles, $\langle \delta r_A^2 \rangle$, showing subdiffusive behavior within the marked intervals. At long times, the diffusive behavior $\langle \delta r_A^2 \rangle \sim t$ is recovered.

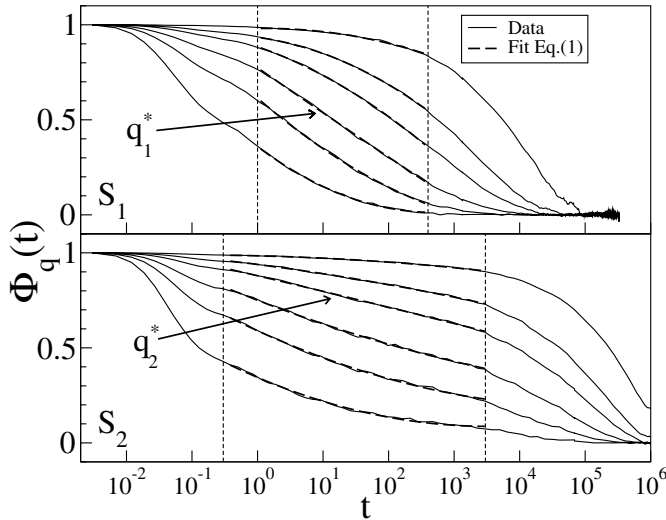


FIG. 3. A-type particle density correlators for S_1 (top panel) and S_2 (bottom panel), showing six different wave vectors (from top to bottom $q\sigma_{BB} = 6.7, 11.7, 16.8, 23.5, 33.5,$ and 50.3). For correlators indicated by an arrow, a logarithmic behavior is observed within the selected time window. The dashed lines show the fits according to Eq. (1). The vertical dashed lines indicate the fitting interval.

To show that the above described features are consistent with the ones predicted by MCT, we cite the general asymptotic decay law for the correlation function of a generic variable X , near the higher-order singularity [17]

$$\Phi_X(t) = f_X - h_X [B^{(1)} \ln(t/\tau) + B^{(2)} \ln^2(t/\tau)]. \quad (1)$$

Here τ abbreviates a time scale which diverges if the state approaches the singularity. The formula is obtained by asymptotic solution of the MCT equations, using the parameter differences $\phi^* - \phi$, $\theta^* - \theta$, $\Delta^* - \Delta$ as small quantities, say, of order ϵ . The coefficient $B^{(1)}$ is of order $\sqrt{\epsilon}$, while $B^{(2)}$ is of order ϵ . The amplitude h_X is independent of ϵ . The first term f_X is the sum of the non-ergodicity parameter of variable X at the singularity and a correction of order ϵ . Terms of order $\epsilon^{3/2}$ are neglected [17]. We can interpret $\ln\langle\delta r_A^2\rangle$ also according to Eq. (1). Hence, the straight line for S_1 with slope a_1 shown in Fig. 2 is consistent with the assumption that S_1 is close to the singularity. Changing from S_1 to S_2 , the slope $a = h_{\text{MSD}} B^{(1)}$ has to decrease and the range of validity of the leading order description has to expand. This is demonstrated impressively by the data.

To estimate the possibility of describing the time dependence of $\Phi_q(t)$ according to Eq. (1), we fit the density autocorrelation functions to a quadratic polynomial in $\ln(t/\tau)$ for different q values. Fits are reported in Fig. 3. The fitting time window extends from about 2.5 decades for the state point S_1 to 4 decades for S_2 . The fitting parameter f_q , shown in Fig. 4, provides an estimate of the nonergodicity parameter at the A_4 point. We find that f_q does not depend on the state point. This

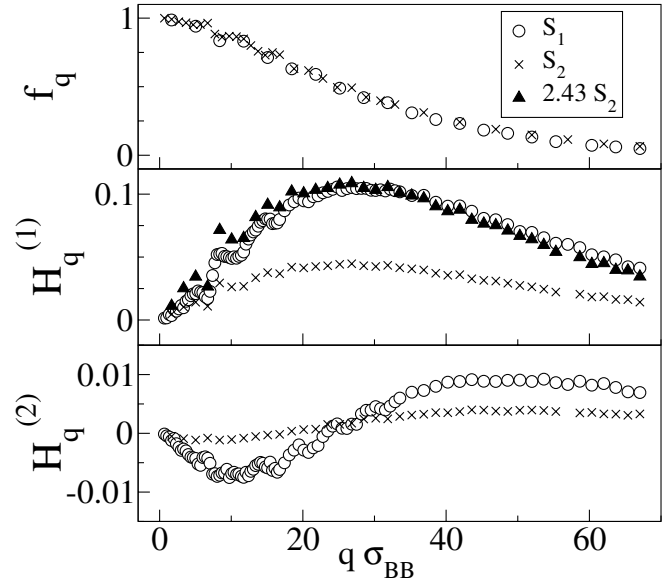


FIG. 4. The fitting parameters f_q , $H_q^{(1)}$, and $H_q^{(2)}$ of the asymptotic logarithmic law, for S_1 and S_2 . The central panel also shows that a multiplication by 2.43 of $H_q^{(1)}$ for the S_2 system gives $H_q^{(1)}$ for S_1 , confirming the factorization of $H_q^{(1)}$. At the wave vector where $H_q^{(2)} = 0$ ($q_2^*\sigma_{BB} = 23.5$ for S_1 and $q_2^*\sigma_{BB} = 16.8$ for S_2) correlation functions display a pure logarithmic decay.

confirms the preceding conclusion that the studied state points are very close to the singularity and that the order ϵ correction in f_q cannot be detected.

The fit parameters for the coefficient $H_q^{(1)} \equiv h_q B^{(1)}$ are reported in the middle panel of Fig. 4. The decrease of $H_q^{(1)}$ upon changing from S_1 to S_2 is in agreement with the prediction that $B^{(1)}$ tends to zero with ϵ approaching zero. As shown in Eq. (1), $H_q^{(1)}$ factorizes into a control-parameter independent factor h_q , depending on q , and a control-parameter dependent factor $B^{(1)}$, independent of q . This implies that the q dependence of $H_q^{(1)}$ should be the same for S_1 and S_2 . As shown in Fig. 4, this property is verified by the data. The same property does not apply to $H_q^{(2)} \equiv h_q B_q^{(2)}$ because of the q dependence of $B_q^{(2)}$. Moreover, the fitting results confirm that $H_q^{(2)}$ is smaller than $H_q^{(1)}$, as expected being the first of order ϵ and the second of order $\sqrt{\epsilon}$. The wave-vector value where $B_q^{(2)} = 0$ allows one to identify the characteristic length scale associated with the pure logarithmic decay (see Fig. 3). Such length scales are much shorter than the typical first neighbor shell.

To explicitly test the mentioned factorization, Fig. 5 shows a set of correlators rescaled to $\hat{\Phi}_q(t) = [\Phi_q(t) - f_q]/H_q^{(1)}$. MCT predicts that in leading order ϵ all $\hat{\Phi}_q(t)$ vs $\ln(t)$ curves collapse on the logarithmic decay law $-\ln(t/\tau)$. This is, indeed, shown for a large time interval that expands upon approaching the singularity, as it is demonstrated by comparing results for S_1 and S_2 [23].

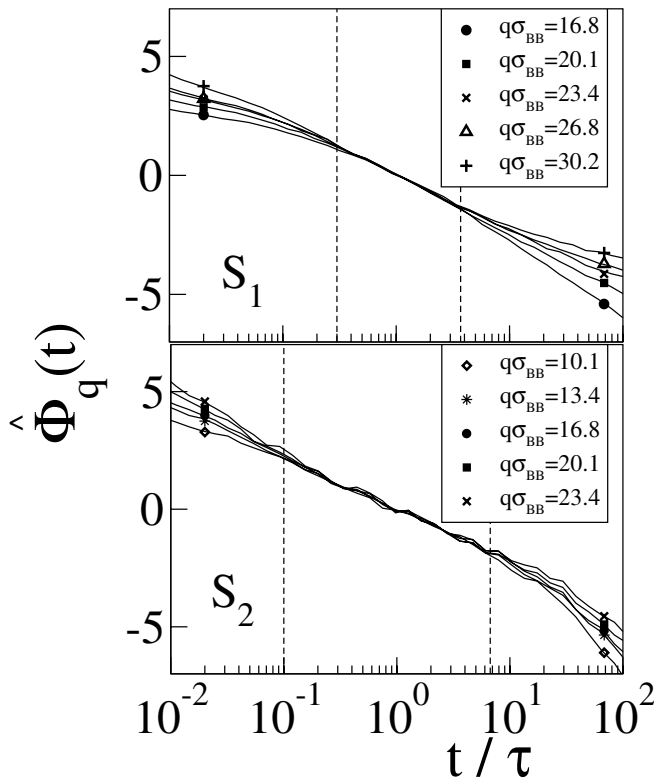


FIG. 5. Scaled correlation functions $\hat{\Phi}_q(t)$ (see text) vs $\ln(t/\tau)$ for the two samples and selected values of $q\sigma_B$ around the characteristic values q^* for which $H_q^{(2)}$ is close to zero. The vertical dashed lines indicate the time interval over which the scaling is observed. The values of τ are 10 and 10^2 for S_1 and S_2 , respectively.

Results reported in this Letter have an intrinsic value associated with the observation, in a particularly simple system—a square-well potential—of a particularly complex dynamics over more than 4 decades in time. They show that MCT, a theory essentially developed to address the problem of the excluded volume glass transition is able—without any modification—to handle the logarithmic dynamics and to provide an interpretative scheme in terms of the A_4 point. The numerical results and the comparison with the theoretical predictions do constitute, in fact, a stringent verification that the logarithmic dynamics in the density autocorrelation functions and the subdiffusive behavior in the MSD can be fully rationalized by MCT. Indeed, data in Figs. 3 and 4 are in agreement with MCT predictions (Figs. 12 and 13 of Ref. [18]). The simplicity of the model and the complexity of the dynamics suggest that the short-range attractive colloids have the potentiality to become a benchmark for the development of extended theories of the glass transition.

We acknowledge support from MIUR PRIN and FIRB and INFN PRA-GENFDT. We thank W. Götze for illuminating discussions, G. Foffi and M. Sperl for com-

ments, and S. Buldyrev for providing us with the molecular dynamics code for square-well binary systems.

- [1] F. Sciortino, *Nature Mater.* **1**, 145 (2002).
- [2] D. Frenkel, *Science* **296**, 65 (2002).
- [3] Articles in *Nonequilibrium Behavior of Colloidal Dispersions*, Faraday Discuss. **123** (2003).
- [4] L. Fabbian, W. Götze, F. Sciortino, P. Tartaglia, and F. Thiery, *Phys. Rev. E* **59**, R1347 (1999); *Phys. Rev. E* **60**, 2430 (1999).
- [5] J. Bergenholtz and M. Fuchs, *Phys. Rev. E* **59**, 5706 (1999).
- [6] K. A. Dawson, G. Foffi, M. Fuchs, W. Götze, F. Sciortino, M. Sperl, P. Tartaglia, Th. Voigtmann, and E. Zaccarelli, *Phys. Rev. E* **63**, 011401 (2001).
- [7] F. Mallamace, P. Gambadauro, N. Micali, P. Tartaglia, C. Liao, and S. H. Chen, *Phys. Rev. Lett.* **84**, 5431 (2000).
- [8] W. R. Chen, S. H. Chen, and F. Mallamace, *Phys. Rev. E*, **66**, 021403 (2002).
- [9] K. N. Pham, A. M. Puertas, J. Bergenholtz, S. U. Egelhaaf, A. Moussaid, P. N. Pusey, A. B. Schofield, M. E. Cates, M. Fuchs, and W. C. Poon, *Science* **296**, 104 (2002).
- [10] T. Eckert and E. Bartsch, *Phys. Rev. Lett.* **89**, 125701 (2002).
- [11] A. M. Puertas, M. Fuchs, and M. E. Cates, *Phys. Rev. Lett.* **88**, 098301 (2002).
- [12] A. M. Puertas, M. Fuchs, and M. E. Cates, *Phys. Rev. E* **67**, 031406 (2003).
- [13] G. Foffi, K. A. Dawson, S. Buldyrev, F. Sciortino, E. Zaccarelli, and P. Tartaglia, *Phys. Rev. E* **65**, 050802 (2002).
- [14] E. Zaccarelli, G. Foffi, K. A. Dawson, S. V. Buldyrev, F. Sciortino, and P. Tartaglia, *Phys. Rev. E* **66**, 041402 (2002).
- [15] E. Zaccarelli, G. Foffi, F. Sciortino, and P. Tartaglia, *Phys. Rev. Lett.* **91**, 108301 (2003).
- [16] W. Götze, in *Liquids, Freezing and the Glass Transition*, edited by J. P. Hansen, D. Levesque, and J. Zinn-Justin (North-Holland, Amsterdam, 1991), p. 287.
- [17] W. Götze and M. Sperl, *Phys. Rev. E* **66**, 011405 (2002).
- [18] M. Sperl, *Phys. Rev. E* **68**, 031405 (2003).
- [19] Distances are in units of σ_B , energy and T in units of u_0 ($k_B = 1$). Time is in units of $\sigma_B(m/u_0)^{1/2}$, mass of m .
- [20] T. Gleim, W. Kob, and K. Binder, *Phys. Rev. Lett.* **81**, 4404 (1998).
- [21] We have solved the Ornstein-Zernike equation on a grid of 20 000 q values, with mesh 0.314 159 3 and the MCT equations on a grid of 2000 q with the same mesh.
- [22] Equilibrium simulations at state points closer to the A_4 point are not feasible with the present computational resources. Present data requested several months of cpu time on a beowulf Athlon cluster.
- [23] All curves should have the same tangent for $t = \tau$ but, to order ϵ , be either convex or concave depending on the sign of $B_q^{(2)}$. This important signature of a higher-order glass-transition singularity is exhibited by the data.